12th International Conference on Fracture Mechanics of Concrete and Concrete Structures
FraMCoS-12
B.L.A. Pichler, Ch. Hellmich, P. Preinstorfer (Eds)

https://doi.org/10.21012/FC12.1119
MS13-1:3

COMPREHENSIVE UNCERTAINTY QUANTIFICATION OF DAMAGE-BASED MODELING OF CRACKING IN REINFORCED CONCRETE STRUCTURES

HEND AL ELANI [1,2], DAVID BOUHJITI[2], LUDOVIC JASON[1], BENJAMIN RICHARD[3]

[1] Université Paris-Saclay, CEA, Service d'Études Mécaniques et Thermiques, 91191, Gif-sur-Yvette, France
[2] ASNR/PSN-EXP/SES/LMAPS, 92262, Fontenay-aux-Roses, France
[3] ASNR/PSN-EXP/SES/B2EM, 92262, Fontenay-aux-Roses, France
hend.alelani@cea.fr

Keywords: Uncertainty quantification, Representative structural volume, Sensitivity analysis, Damage, Cracking

Abstract: This work addresses the uncertainties inherent in civil engineering, arising from various sources such as the spatiotemporal variations in material properties, the complexity of concrete behavior, variations in applied loads and the impreciseness of theoretical models. This research aims to explore the advantages of accounting for some uncertain parameters in the numerical damage-based modeling of cracking in reinforced concrete structures, specifically investigating their impact on the accuracy and reliability of simulated outputs. By accounting for these uncertainties, the study aims to improve the predictive capability of numerical models, resulting in simulated responses that align more closely with observed on-site behavior.

To achieve this aim, a case study involving a Representative Structural Volume (RSV) of a part of a 1450MWe nuclear power plant containment building is considered. It is based on the PACE-1450 experimental campaign [1], which aims to thoroughly characterize cracking and air flow through these cracks for various tensile loads and temperatures. Experimental results show strong asymmetric cracking even though the applied tensile loads are mostly unidirectional using hydraulic jacks.

To accurately represent the experimental distribution of the cracking pattern, several input parameters including material properties and boundary conditions during testing are considered as uncertain. The spatial variability of concrete properties is described using discretized random fields associated with the tensile strength [2]. In addition, uncertainties are considered in the angle of application of tensile loads applied via hydraulic jacks, which are suspected to deviate slightly from the surface normal rather than being perfectly perpendicular. These deviations may significantly influence the observed cracking behavior.

First, a sensitivity analysis is performed to identify the most influential input parameters on the computed cracking patterns. Second, based on the obtained results, an attempt is made to determine the set of input parameters that replicate the observed cracking patterns.

The obtained results highlight the critical need for comprehensive uncertainties quantification to objectively assess the results of complex experimental campaigns. They also indicate that accounting for random uncertainty alone is insufficient to replicate the experimental results. Indeed, considering the epistemic uncertainty is needed, particularly regarding the boundary and loading for a comprehensive consideration of uncertainties and better understanding of the observed behavior.

1 INTRODUCTION

Despite recent advances in computational models, they still provide an idealized representation of reality, especially when applied to massive and complex structures like nuclear containment buildings (NCBs). These structures require numerous input parameters, including thermo-hydro-mechanical material properties, structural geometry, boundary conditions, and other factors that inherently possess uncertainties. These uncertainties present significant challenges in accurately assessing their structural and functional performance, such as aging, cracking, long-term operations management and containment properties.

On the matter of spatiotemporal variation of concrete properties, one way to address the issue in numerical models is to use random fields associated with parameters defining the cracking patterns such as tensile strength, fracture energy, and Young's modulus. This has the advantage of being a non-intrusive process that is compatible with all scales of modeling including the macroscopic one, which is mostly used for large structures modeling to keep the computational time reasonable. However, this only describes a part of the overall uncertainties; other ones might be as influential if not more on the observed response and should not be overlooked. This includes accounting for uncertainties on boundary conditions and applied loads.

To highlight the combined effect of these two sources of uncertainties, the case of a RSV within the standard zone (PACE) of a NCB is considered hereafter. It draws from the findings of the PACE-1450 experimental campaign [1], which aimed to investigate the behavior of prestressed and reinforced concrete in the containment building of a 1450 MWe nuclear power plant. The experimental results demonstrated asymmetric and irregular cracking under macroscopic and supposedly homogeneous unidirectional tensioning applied through installed hydraulic jacks.

Consequently, to replicate the observed cracking patterns during the tensile tests on the RSV, discretized random fields associated with tensile strength have been generated.

Additionally, a sensitivity analysis was performed to distinguish the respective contributions of spatial randomness in concrete properties, uncertainties in other material properties, and the applied boundary conditions during testing. Particular attention was given to the misalignment of hydraulic jacks, with the goal of evaluating their impact on the model's output, specifically in terms of the number of cracks and their spatial distribution.

2 DESCRIPTION OF THE PACE-1450 EXPERIMENTAL CAMPAIGN

The PACE ("PArtie Courante de l'Enceinte") mock-up, [1], is a collaborative research action between the EDF R&D department and MPA Karlsruhe. It focuses on studying the RSV within the standard zone in the inner wall of a double-walled nuclear containment building (see Figure 1). Specifically, the PACE-1450 experiment examines the behavior of a curved wall with dimensions of 3.5 m (length), 1.8 m (height), and 1.2 m (width), representing a 1450 MWe nuclear power plant containment under defined accidental loading conditions. The experimental campaign was designed to simulate aging effects through the gradual loss of prestressing, where a controlled reduction in prestressing was implemented during the campaign to accelerate the effects of concrete creep and its influence on the post-tensioning system. While drying and shrinkage are natural long-term phenomena in concrete, their effects were indirectly simulated through this gradual decrease in prestressing force.

To simulate the tensile state in the containment building under accidental inner pressure, hydraulic jacks were installed on the mock-up to induce direct tensile loads on the lateral edges of the RSV. The load by the hydraulic jacks was increased in a continuous way to develop progressively cracks and monitor crack initiation and propagation through the experimental tests. Another aspect of the experimental program, which will not be

detailed hereafter, is related to the measurement of air leakage through created cracks under dry air, heated air and heated air-steam mix.

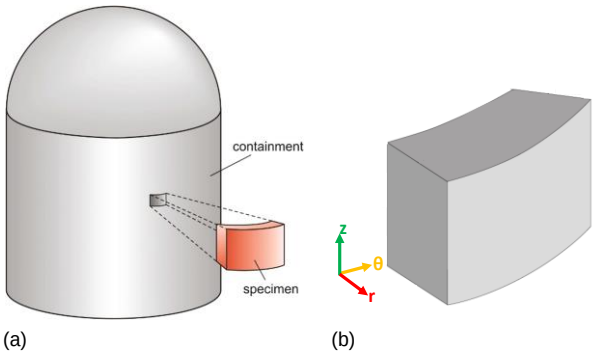

Figure 1 : (a) The specimen is a portion of the cylindrical part of the containment [3]; (b): Orientation of the specimen in cylindrical coordinates.

The reinforcement layout is very similar to the original geometry of the studied NCB, where it consists of meshes of bars near the inner and outer surfaces (refer to Figure 2 & Figure 3).

Additionally, prestressing cables are used, with one vertical prestressing cable oriented in the z-direction and four circumferential prestressing cables oriented in the θ-direction, [4]. In the circumferential direction, the concrete specimen is post-tensioned using four tendons, each comprising 37 strands, with tension adjusted to maintain a stress state of 12 MPa. To account for the prestressing losses due to creep and shrinkage, the level of prestressing in the θ-direction is progressively reduced for several experimental runs. Initially, the prestressing level is set at 12 MPa (100%). It is then reduced to 9.6 MPa (80%), and further to 7.2 MPa (60%). In the vertical direction, for installation purposes, the cable is not tensioned, while steel cushions have been used to ensure a 1MPa compressive stress in the vertical direction of the NCB. This is also a non-representative boundary condition, compared to on-site building, since the prestressing load is around 8 MPa for real full-scale nuclear containment buildings.

The experimental setup is shown in Figure 4. It primarily includes the post-tensioned specimen itself, inner abutments, steel beams

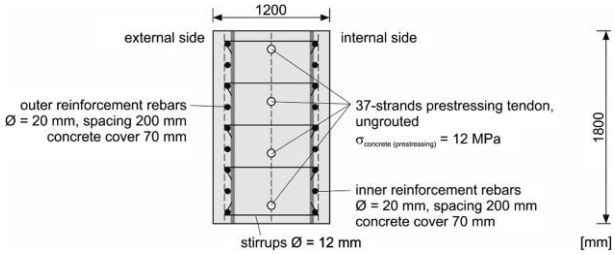

Figure 2 : Cross-section of the specimen as part of the containment (side view) [4]

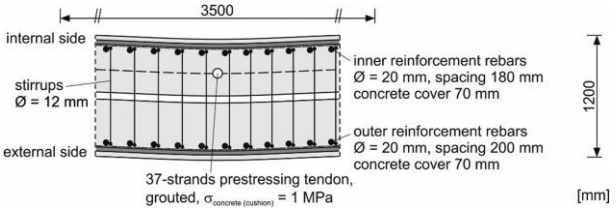

Figure 3: Vertical section in the longitudinal direction of the specimen (top view) [4]

(referred to as "ears") on both left and right sides, and hydraulic jacks that push the ears outward. Additionally, the setup comprises the pressure chamber, which doubles as a cover atop the specimen, as well as the foundations for the specimen, and the abutments to complete the mechanical setup, allowing for the replication of the loading conditions of a real NCB.

In terms of external loads and in addition to the prestressing in cables, the specimen is

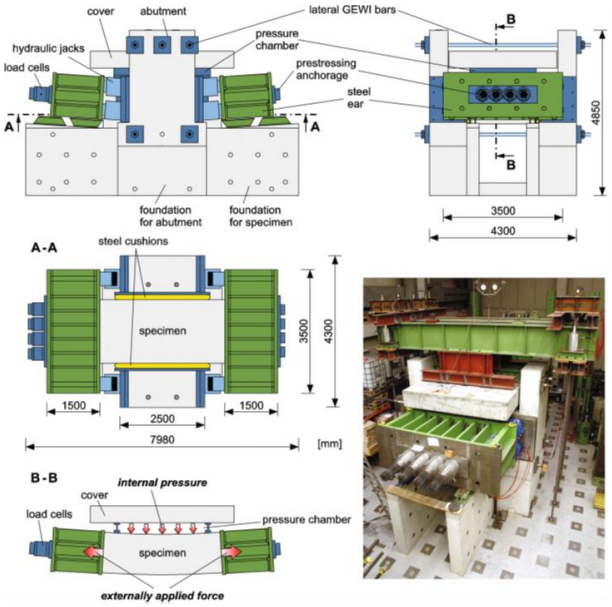

Figure 4 Drawings of the mechanical part of the facility (in section B-B the applied force is shown in principle) and photo of the mechanical set-up [4]

subjected to pressures simulating accidental containment conditions of up to 6 bars (all pressure values in this paper are given in absolute terms) that are obtained with the help of the pressure chamber atop of the specimen. (see Figure 4).

In total, 12 RUNs have been conducted with tensile stresses emerging for the first time in RUN3 with a prestressing level of 60%, a pressure level of 5.3 bars, and a total hydraulic jacks load of 4238kN (this is equivalent to a tangential stress of 7.85MPa). Then at RUN4 (prestressing level, a total hydraulic jack load remains the same, while the pressure level was incremented up to 6 bars to simulate the accidental containment conditions). One observes a permanent cracking pattern with four main through cracks on the right side and none on the left side (red lines in Figure 5).

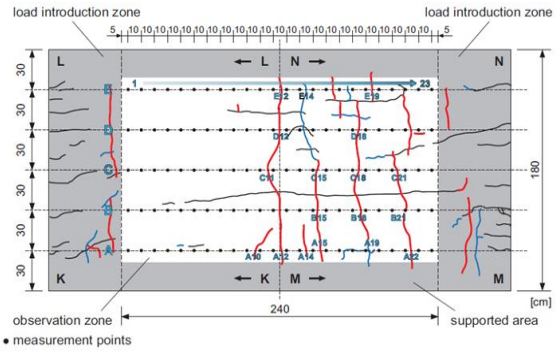

Figure 5 : Cracking pattern on the external side of the specimen during RUN4 [5]

Some cracks nearby the edges have been observed as well but they were simply coated so as not to disturb the airflow through the rest of the cracks in the central observation area.

3 DESCRIPTION OF THE NUMERICAL MODEL OF THE PACE-1450

3.1 Geometry and mesh

The geometry of the specimen is derived from the definition of the experimental campaign (3.5m× 1.8m× 1.2m). Figure 6(a) illustrates the dimensions of the RSV in the original orientation as a portion of the containment wall, while Figure 6(b) presents the specimen's orientation in the laboratory. One can note that the dead load is not acting in the same direction for both configurations (Figure 6(a) and Figure 6(b)), where the dead load in the real containment building configuration (Figure 6(a)) is along the z-direction, while in the laboratory configuration Figure 6(b)) is along the central radial direction. However, this should have a limited impact on the obtained cracking patterns. Surface definitions have been established based on the original orientation (see Figure 6(c)). The concrete is represented using volumetric finite elements, while the reinforcement (presented in Figure 2 & Figure 3) and prestressed cables (refer to Figure 6(a)) are represented using bar elements. A perfect steel-concrete bond is assumed for the interaction between these components. The model's meshing process involves a perfect nodal correspondence between steel elements (cables, stirrups and rebars) and concrete elements. All mesh elements used are linear, consisting of quadrilateral faces for surface elements and hexahedral volumes for solid functions.

To assess the accuracy and convergence of the numerical simulations, two different mesh densities were employed for the concrete specimen: a coarse mesh and a refined mesh. The coarse mesh, with fewer elements, is used for initial, computationally efficient simulations, while the refined mesh, containing a higher number of elements, provides greater accuracy by capturing more detailed stress and strain distributions. Figure 7 illustrates the coarse and refined mesh configurations, highlighting the differences in element size and distribution used in the analysis. These variations allow for a comparative study of the impact of mesh resolution on the results.

3.2 Boundary conditions

In terms of boundary conditions, radial displacement has been restricted at the extrados' side edges touching the support, where these side edges are free to move in the negative radial direction but are constrained in the positive radial direction (see Figure 8). Additionally, the normal displacement (i.e., the displacement in the θ-direction) is restrained

on the right lateral surface (SR). The vertical displacement (in the z- direction) is constrained at point (P0), positioned near the bottom of the right lateral surface (refer to Figure 8). To avoid surface twisting, which would lead to torsional stresses that are not present in the real mock-up, a uniform displacement constraint is applied in the normal direction on the left lateral surface (SL). These boundary conditions are sufficient to guarantee that the mechanical problem is well posed from a numerical perspective.

3.3 Mechanical loading conditions

To simulate the various loads applied to the PACE-1450 mock-up, the following loading conditions were implemented in the PACE-1450 numerical model:

- **Dead load:** This includes the self-weight of the concrete, reinforcement, and cables applied along to the central radial direction.
- **Vertical prestressing cable:** A constant vertical prestressing pressure was applied using steel cushions on both the top (SH) and bottom (SB) surfaces. It was modeled as pressure acting on both surfaces (SH & SB). This simulates the effect of the vertical cable in the NCB.
- **Circumferential prestressing cables:** The circumferential prestressing forces provided by the four cables were simplified by modeling them as a pressure applied uniformly on the left lateral surfaces (SL). This approach allows us to simulate the effect of circumferential prestressing in the NCB without requiring detailed modeling of each individual cable and its interactions, thereby reducing model complexity and computational cost.
- **Tensile force applied through hydraulic jacks:** The tensile force generated by hydraulic jacks (HJ), was also modeled as a negative pressure (tensile stress) in the circumferential / ortho-radial direction, applied on the left lateral surfaces (SL) of the specimen. This approach effectively simulates the ring tensile stresses induced by internal pressure within the NCB. This modeling choice aligns with the mechanical setup, in which hydraulic jacks push the steel beams, or "ears," outward, creating a uniform distribution of the applied forces across the lateral surfaces; SL, and SR (refer to Figure 4).
- **Internal pressure:** The pressure exerted by the chamber positioned atop the specimen, was modeled as a radial pressure applied on the intrados (SI). It simulates the internal pressure in the NCB.

As discussed in section 2, various RUNs have been done, each with specific loading conditions. For this study, RUN 4 was analyzed, during which four cracks propagated in the specimen. Thus, the loading conditions adopted for this study, are based on RUN 4. Figure 9 shows the resultant prestressing pressures due to the four cables in the circumferential direction (θ-direction) and the one cable in the vertical direction (z-direction). Figure 10 illustrates the variation in internal pressure within the top chamber over time, along with the variation in ring tensile stress (denoted by HJ equivalent stress in Figure 10) simulated through force applied by means of hydraulic jacks, as previously mentioned.

3.4 Mechanical Behavior of Materials

The mechanical behavior of concrete is simulated using the regularized Mazars constitutive law ([6],[7]) in Cast3M software[8]. This damage-based model characterizes cracking as a progressive loss of stiffness governed by a softening law, ensuring compliance with a specific fracture energy criterion under tensile loading. The damage variable ranges from 0 for sound concrete to 1 for a totally damaged element. The model allows for some residual strength for totally damaged elements (around 5%) and does not account for irreversible strains. Although the model considers damage under compressive loads, this aspect is not engaged in the present case, as the specimen remains elastic in the compression domain. This is because the applied compressive loads did not reach thresholds that would initiate compressive

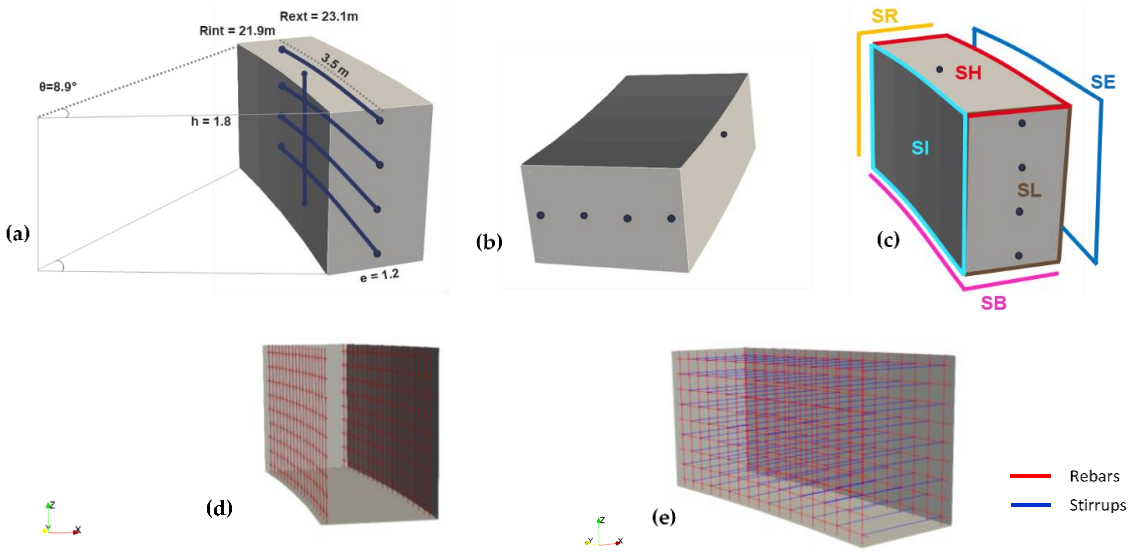

Figure 6 : (a): Specimen geometry as part of the containment and cable positioning overview, (b): Specimen orientation in the laboratory, (c): Definition of the six surfaces of the specimen, (d): Inner and outer rebars, (e): Stirrups.

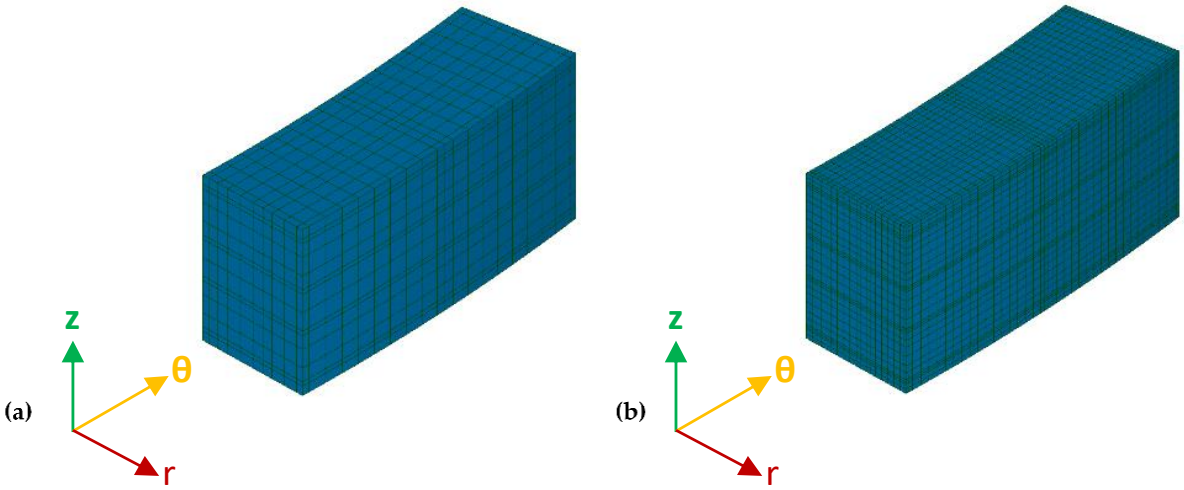

Figure 7 : (a): Coarse mesh and (b): Refined configurations of the concrete specimen.

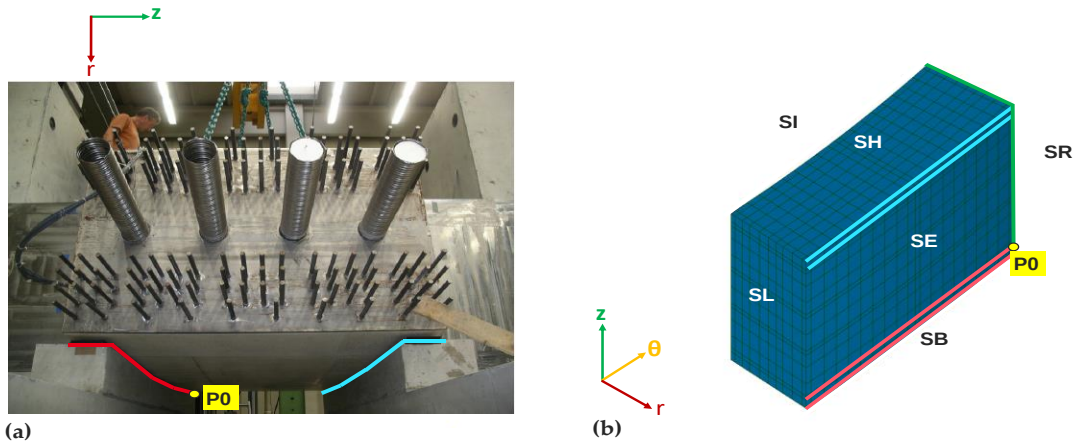

Figure 8 : (a): Specimen being set onto the foundations between the abutments (Modified from [5]), (b): Visual representation of boundary conditions.

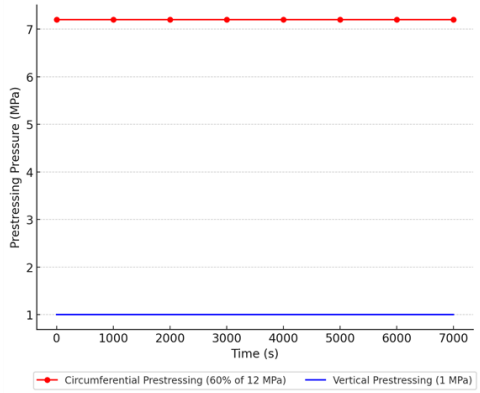

Figure 9 : Prestressing pressure over time for RUN 4.

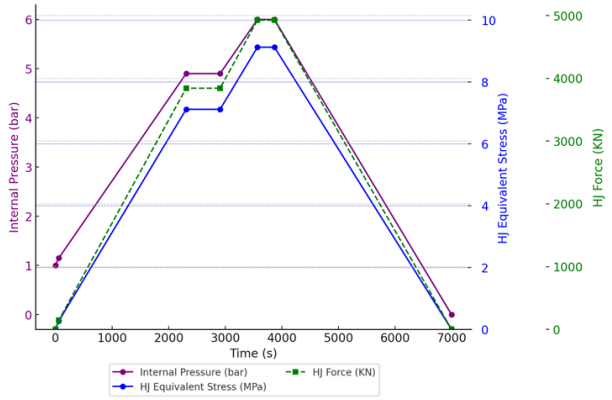

Figure 10 : Internal pressure, HJ force and HJ equivalent applied stress scenarios for RUN 4.

damage [9].

The input parameters for concrete material in this model are divided into two categories. The first category includes constant parameters such as Poisson's ratio (ν = 0.25), fracture energy (G_F = 100 N/m), and concrete density (ρ = 2339 kg/m³). The second category consists of uncertain parameters, including Young's modulus (E), ranging from 14 GPa to 26 GPa, and tensile strength (ft), ranging from 1.3 MPa to 2.5 MPa. This variability reflects the intrinsic nature of size effects phenomena, which influence the nominal strength of concrete based on the volume subjected to tensile loads [10]. In concrete, the size effect is linked to the heterogeneity of the material. Since concrete is a composite of aggregates, cement, and voids, larger specimens are more likely to contain larger and more critical flaws that can compromise strength [11]. In quasi-brittle materials like concrete, size effect is also due to the micro-cracking induced by autogenous shrinkage of the cement paste around aggregates [12].

The parameters of Mazars model are defined to have a softening curve meeting the Hillerborg [7] energy-based criterion of energy dissipation based on the characteristic length *lc* of the finite elements (refer to equation (1)).

$$\frac{G_F}{lc} = \int_0^{+\infty} \sigma(\varepsilon) d\varepsilon \qquad (1)$$

For steel elements, including reinforcement bars and prestressing cables, an elastic behavior model is applied, as no yielding was observed during the experimental RUNs. The steel is characterized by a Young's modulus of 210 GPa, a Poisson's ratio of 0.28, and a density of 7850 kg/m³. Furthermore, the potential for yielding in the simulation was evaluated, and the results confirmed that the stress levels in the steel remained below the yield strength, ensuring that yielding did not occur in the simulated conditions.

3.5 Accounting for Uncertainties

In this work, the spatial variability of concrete properties, specifically, the tensile strength, is treated as an aleatoric uncertainty. This type of uncertainty, inherent in the material properties due to natural variability, is commonly addressed in civil engineering probabilistic modeling. To capture this variability within the PACE-1450 numerical model, a random field approach is employed, representing the heterogeneous distribution of tensile strength across the concrete specimen. The random field is generated through the damage strain threshold (ε_0), with the mean value of ε_0 set to the mean value of ft over the mean value of E (equation (2)). This approach allows the tensile strength to vary spatially while maintaining homogeneity in the elastic modulus (E), which is assigned a constant mean value across the specimen. The resulting strain field is then scaled by the mean value of E, ensuring that only tensile strength is treated as a spatially variable property, while E remains uniformly distributed across the specimen. This

method is particularly suited to capture the effects of material heterogeneity on crack initiation and propagation in concrete structures.

$$\mathbb{E}[\varepsilon_0] = \frac{\mathbb{E}[ft]}{\mathbb{E}[E]} \quad (2)$$

The random field itself is generated using the Turning Band Method, as implemented in Cast3M [8]. This method creates an isotropic random field with an exponential covariance function (refer to equation (3)), characterized by a specified mean, standard deviation (σ), and correlation length. Due to the isotropic assumption, the correlation length remains identical in all directions ($l_1 = l_2 = l_3$). The covariance function depends also on the spatial separation between two points, represented by d_1, d_2, d_3, which correspond to the coordinate differences between two mesh points along the three spatial directions. By introducing a random field for tensile strength, this approach provides a more realistic representation of the stochastic nature of concrete, allowing for a probabilistic analysis of cracking behavior that can account for variations in material strength across the specimen.

$$C_{ij} = \sigma^2 \, exp\left(-\sqrt{\frac{d_1^2}{l_1^2} + \frac{d_2^2}{l_2^2} + \frac{d_3^2}{l_3^2}}\right) \quad (3)$$

However, this approach addresses only part of the overall uncertainties; other sources of uncertainty, such as boundary conditions and applied loads, may also significantly influence the observed response and should not be neglected. These additional uncertainties could have an impact comparable to, or even greater than, that of spatial variability, highlighting the importance of a comprehensive uncertainty quantification strategy.

Consequently, in this work, the alignment of hydraulic jacks applying the ortho-radial tensile loads (see Figure 11) is considered as an epistemic uncertainty. During the experiments, it is plausible that some degrees of misalignment (denoted as angle α) occurred, which may have contributed to the asymmetric cracking patterns observed in . Therefore, the hydraulic jacks applying tensile loads are assumed to be misaligned on one of the lateral surfaces (the left surface SL is considered) of the specimen. This misalignment implies that the jacks are no longer perfectly perpendicular to the surface; instead, they form an angle α with respect to the normal of the lateral surface. As a result, the applied tensile stress (HJ equivalent stress) on this lateral surface will be decomposed into two components:

1. A component in the ortho-radial (θ-direction), which is the cosine of angle α multiplied by the resultant applied tensile stress (illustrated by the yellow arrows on the left side of the specimen).
2. A component in the radial (r-direction), which is the sine of angle α multiplied by the resultant applied tensile stress (illustrated by the red arrows on the left side of the specimen).

Thus, the consideration of both aleatoric and epistemic uncertainties highlights the importance of accounting for various sources of variability to improve the understanding and prediction of concrete structures' behavior under load. To identify the most influential parameters among these uncertainties, a sensitivity analysis should first be performed. This would allow for a focused exploration of critical factors whose variation significantly influences the specimen response.

3.6 Sensitivity analysis

The Hilbert-Schmidt Independence Criterion (HSIC) method has been employed to identify the most influential parameters affecting the variation in both the number and distribution of cracks in the extrados. The HSIC method is a statistical approach used to measure the dependency between multiple variables, allowing for the identification of which input parameters have the greatest impact on a specific output, which is a characteristic of cracking pattern in this case. HSIC sensitivity indices include two components: 1-p-value and R^2HSIC. The 1-p-value is particularly efficient for identifying influential parameters, serving as a screening tool, while the R^2HSIC value offers a quantitative measure of dependency

strength, allowing for a ranking of inputs from most to least influential. However, since the primary objective of this sensitivity analysis is to distinguish influential parameters from non-influential ones, the focus is placed on the 1-p value for this type of screening analysis, as it directly assesses statistical significance.

This method provides a robust means of understanding the sensitivity of the crack patterns to different variables, ultimately aiding in reducing the dimension of the probabilistic problem by detecting the critical parameters that highly contribute to the model's output. Sensitivity analyses conducted in this section have been done using URANIE software [13], [14], coupled with the FEM software Cast3M [8]. Both software programs are developed by CEA.

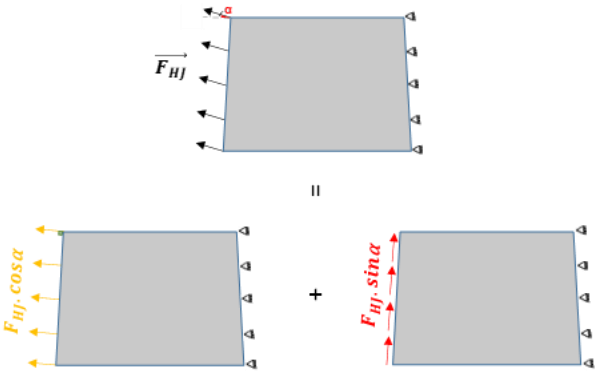

Figure 11: Illustration of hydraulic jacks Inclination with an angle α

Two sensitivity analyses were performed in this section: the first without and the second with random field generation. The objective is to check the influence of different inputs on the number and distribution of cracks along the outer surface of the specimen (extrados). In this context, the terms "Left," "Middle," and "Right" refer to the spatial zones on the extrados of the specimen where cracks are counted. The Middle Zone encompasses the region spanning 10 cm to the left and 10 cm to the right of the extrados' centerline. The Left Zone extends from the left border of the Middle Zone to the edge of the extrados, while the Right zone extends from the right border of the Middle Zone to the opposite edge. The crack counts in these three regions are determined by analyzing the damage variable and strain values extracted from the nodes along a predefined curved line located on the extrados of the FEM. The position of this line was selected based on insights gained from multiple simulation runs to ensure it captures the critical cracking behavior. A crack is identified at a specific position if the nodal damage variable exceeds a defined threshold, set to 0.6 in this analysis. This criterion provides a consistent and quantitative method for identifying and counting cracks, reflecting the degree of material degradation on the extrados.

To comprehensively explore the variability of input parameters influencing the cracking process, a numerical design plan was adopted, as summarized in Table 1. This table outlines the variation domain of each input variable, along with their respective distributions and underlying objectives.

The selected variation domains for Young's modulus and tensile strength reflect the intrinsic nature of size effects in concrete, which influence its nominal strength based on the volume subjected to tensile loads [10]. Young's modulus varied within [14 GPa, 26 GPa], while tensile strength was considered in the range [1.3 MPa, 2.5 MPa]. This variability accounts for the heterogeneity of concrete, a composite material consisting of aggregates, cement, and voids, where larger specimens are more likely to contain larger and more critical flaws that reduce their overall strength [11]. In brittle materials like concrete, the size effect arises primarily due to micro-cracking induced by autogenous shrinkage of the cement paste around aggregates[12]. The hydraulic jack misalignment was considered within [0°, 6°], as epistemic uncertainties related to deviations in loading alignment can significantly impact stress distribution and crack initiation. The correlation length was selected within [0 m, 1.5 m], representing the spatial extent over which mechanical properties exhibit statistical correlation, ensuring that both localized and more widespread variations are accounted for. Lastly, 100 realizations of the random field were generated to investigate the impact of spatial randomness on cracking behavior, ensuring statistical significance in the results.

Table 1 : Variation domains and distributions of input parameters for sensitivity analysis

Input Variables	Aim of Variability	Distributions
Mean Value of Tensile Strength (MPa)	to explore size effect	U[1.3,2.5]
Young's Modulus (GPa)	to explore size effect	U[14,26]
Hydraulic Jacks alignment (°)	to explore epistemic uncertainties effect	U[0,6]
Correlation Length (m)	to explore the size effect	U[0,1.5]
Random Fields Realizations	to explore the spatial randomness effect	Discrete {1,2,…,100}

The initial sensitivity analysis was performed by considering three key uncertain input parameters: tensile strength (ft), Young's modulus (E), and the alignment angle of the hydraulic jacks (α). This analysis was carried out without incorporating random field generation, focusing instead on the global influence of these parameters on the system's response. This approach allows for a preliminary understanding of parameter sensitivity without the added complexity of spatial variability introduced by random fields. The results of this analysis are presented in Figure 12. Based on the 1-pvalues curves shown in Figure 12, influential parameters are identified as those for which 1−p exceeds 95%. When this threshold is met, it indicates that the hypothesis of dissimilarity between the joint distribution of the input-output pair and the product of their marginal distributions is significant. In other words, if 1−pvalue is greater than 0.95, the input and output are considered dependent, implying that the input parameter has an important influence on the output. Therefore, any parameter satisfying this condition is classified as an influential parameter. Consequently, the tensile strength (ft), and the alignment angle of hydraulic jacks (α) are identified as the influential parameters affecting the number of cracks in the left, middle, and right regions of the extrados.

To go further and check for the influence of random field realizations and correlation length, an additional sensitivity analysis was conducted. In this analysis, the parameters identified as influential from the initial sensitivity analysis: tensile strength (ft) and the alignment angle of the hydraulic jacks (α), were included along with random field realizations and correlation length, as uncertain inputs. The results of this analysis are presented in Figure 13. Tensile strength (ft) and the alignment angle of the hydraulic jacks (α) also stand out as crucial parameters.

Physically, this result aligns with expectations, as tensile strength represents the material's inherent resistance to cracking. Meanwhile, the alignment angle directly influences stress distribution, effectively governing the direction and intensity of applied forces.

These findings highlight the interplay between geometric and material factors, emphasizing the importance of both alignment and tensile properties in predicting crack behavior across different regions of the extrados. In contrast, random field realizations (RF) and correlation length (lf) show relatively low (1-p) values across all zones, indicating that the variation of these parameters has limited effect on the crack patterns in this loading case of the model, comparing with other parameters. The low influence of random field realizations and correlation length suggests that while these factors contribute to variability, they do not substantially alter the overall cracking behavior in the extrados.

4 CONCLUSION AND PERSPECTIVES

4.1 Conclusion

The study presented in this paper demonstrates that the value of tensile strength has a more pronounced influence on cracking patterns compared to its spatial variability.

Although spatial variability is essential for capturing the heterogeneous nature of concrete, the findings indicate that, within the

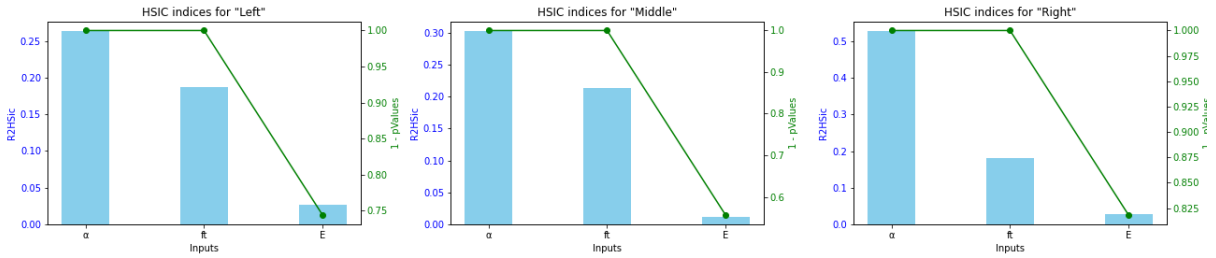

Figure 12: Primary HSIC sensitivity analysis indices for the three regions of the extrados: Left, Middle, and Right

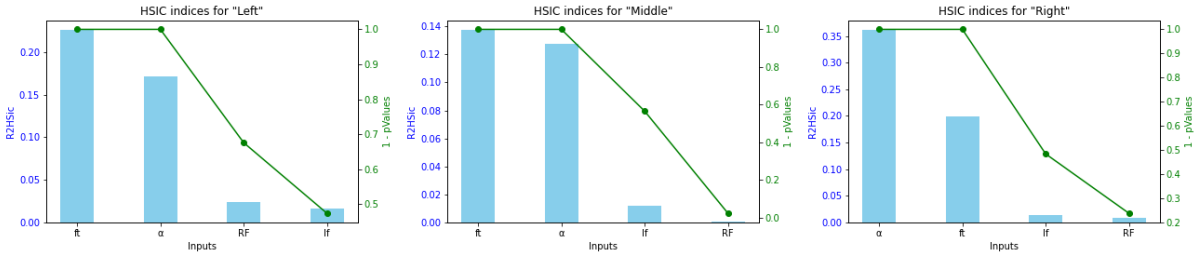

Figure 13: Secondary HSIC sensitivity analysis indices for the three regions of the extrados: Left, Middle, and Right

context of this experimental campaign and the loading conditions of RUN4, changes in spatial discretization have a limited impact on the results within the range of variation of the selected parameters.

In addition, the research highlights the significant impact of epistemic uncertainty, particularly the sensitivity of experimental outcomes to the alignment of loading equipment. Even minor misalignments in the loading setup can cause substantial variations in cracking behavior, emphasizing the critical need for precision in both experimental configurations and numerical simulations. Addressing both aleatoric and epistemic uncertainties within the modeling framework enhances the predictive accuracy and reliability of the models. This comprehensive approach provides a deeper understanding of the observed structural behavior under various loading conditions, ensuring the models are better suited for real-world engineering applications where uncertainties are unavoidable.

4.2 Perspective

At the reduced scale, the PACE-1450 model will be simplified using a surrogate model that focuses on the most influential parameters identified through sensitivity analysis. Bayesian updating will then be applied to integrate experimental data into the surrogate model, thereby improving its predictive accuracy and reducing uncertainties. This iterative process aims to enhance the model's reliability and robustness.

REFERENCES

[1] N. Herrmann, H. S. Müller, S. Michel-Ponnelle, B. Masson, and M. Herve, “The PACE-1450 experiment–investigations regarding crack and leakage behaviour of a pre-stressed concrete containment,” presented at the High Tech Concrete: Where Technology and Engineering Meet: Proceedings of the 2017 fib Symposium, held in Maastricht, The Netherlands, June 12-14, 2017, Springer, 2018, pp. 1487–1495.

[2] D. E.-M. Bouhjiti, J. Baroth, F. Dufour, M. Briffaut, and B. Masson, “Probabilistic analysis of concrete cracking using stochastic finite element methods: application to nuclear containment buildings at early age,” *Mater. Struct.*, vol. 53, no. 4, p. 93, Jul. 2020, doi: 10.1617/s11527-020-01519-3.

[3] N. Herrmann *et al.*, "PACE 1450 - Experimental investigation of the crack behaviour of prestressed concrete containment walls considering the prestressing loss due to aging," Aug. 2009.

[4] N. Herrmann, H. S. Müller, S. Michel-Ponnelle, B. Masson, and M. Herve, "The PACE-1450 Experiment – Investigations Regarding Crack and Leakage Behaviour of a Pre-stressed Concrete Containment," in *High Tech Concrete: Where Technology and Engineering Meet*, D. A. Hordijk and M. Luković, Eds., Cham: Springer International Publishing, 2018, pp. 1487–1495. doi: 10.1007/978-3-319-59471-2_171.

[5] N. Herrmann, H. S. Müller, C. Niklasch, S. Michel-Ponnelle, and B. Masson, "Leakage Behaviour of a Pre-stressed Concrete Containment under Air and Steam Loads in the PACE-1450 Experiment," 2015.

[6] J. Mazars, "Application de la mécanique de l'endommagement au comportement non linéaire et à la rupture du béton de structure," *Thèse Dr. Ès Sci. Présentée À L'Université Pierre Marie Curie - Paris 6*, 1984.

[7] A. Hillerborg, M. Modéer, and P.-E. Petersson, "Analysis of crack formation and crack growth in concrete by means of fracture mechanics and finite elements," *Cem. Concr. Res.*, vol. 6, no. 6, pp. 773–781, Nov. 1976, doi: 10.1016/0008-8846(76)90007-7.

[8] *Cast3M. Code de Calcule aux Eléments Finis CAST3M. Tech rep, Commissariat à l'Energie Atomique, CEA-DES/DM2S/SEMT; 2023.https://www-cast3m.cea.fr/index.php?page=notices&notice=MATE#MECANIQUE%20ENDOMMAGEABLE17.*

[9] H. Kupfer, H. K. Hilsdorf, and H. Rusch, "Behavior of concrete under biaxial stresses," presented at the Journal proceedings, 1969, pp. 656–666.

[10] A. Sellier and A. Millard, "Weakest link and localisation WL ^{2}: a method to conciliate probabilistic and energetic scale effects in numerical models," *Eur. J. Environ. Civ. Eng.*, pp. 1–15, Apr. 2014, doi: 10.1080/19648189.2014.906368.

[11] Z. P. Bazant and M. T. Kazemi, "Size effect on diagonal shear failure of beams without stirrups," *ACI Struct. J.*, vol. 88, no. 3, pp. 268–276, 1991.

[12] F. Bourgeois, N. Burlion, and J. F. Shao, "Modelling of elastoplastic damage in concrete due to desiccation shrinkage," *Int. J. Numer. Anal. Methods Geomech.*, vol. 26, no. 8, pp. 759–774, Jul. 2002, doi: 10.1002/nag.221.

[13] J.-B. Blanchard, G. Damblin, J.-M. Martinez, G. Arnaud, and F. Gaudier, "The Uranie platform: an open-source software for optimisation, meta-modelling and uncertainty analysis," *ArXiv Prepr. ArXiv180310656*, 2018.

[14] URANIE, *URANIE*. (Apr. 09,). CEA.